International Journal of Thermophysics, Vol. 24, No. 5, September 2003 (© 2003)

Experimental Measurements and Theoretical Prediction of the Thermal Conductivity of Two- and Three-Phase Water/Olivine Systems[1]

F. Gori[2,3] and S. Corasaniti[2]

The thermal conductivity of olivine, dry and mixed with water, up to saturation, has been measured with a thermal probe, using the step heating method. The olivine is composed of solid particles with dimensions in the range from 0.8 to 1 mm. Dry olivine has been measured in the range of temperatures between −17° to +50°C. Olivine mixed with water has been measured at +50°C. The cubic cell model has been used to make predictions to compare with the measured data. Comparisons of the experimental thermal conductivities and the predicted values of dry and water-mixed olivine show good agreement. The cubic cell model can be used to evaluate the porosity of olivine and the thermal conductivity of the solid particles, from the values measured at dryness and saturation, with reasonably good agreement. In this way, it is not necessary to measure the mineral composition of the particles of the porous media. Also, the porosity of the medium is predicted with reasonable agreement, which takes into account the phenomenon of the porosity increase near the probe, since the diameter of the probe is smaller than that of the solid particles.

KEY WORDS: cubic cell model; measurement; theoretical prediction; thermal conductivity; thermal probe; water/olivine system.

1. INTRODUCTION

A knowledge of the effective thermal conductivity of porous media is very important in many heat and mass transfer phenomena, including those in

[1] Paper presented at the Sixteenth European Conference on Thermophysical Properties, September 1–4, 2002, London, United Kingdom.

[2] Department of Mechanical Engineering, University of Rome "Tor Vergata," via del Politecnico 1, 00133 Rome, Italy.

[3] To whom correspondence should be addressed. E-mail: gori@uniroma2.it

0195-928X/03/0900-1339/0 © 2003 Plenum Publishing Corporation

soils, either terrestrial or extraterrestrial. Indeed, space exploration needs to know the thermal properties of soils expected on Mars and comets. Direct measurements of the thermal conductivity of Martian soil are lacking, and its values can be inferred only by terrestrial analogues. Measurements of the thermal properties of the Martian soil, such as thermal conductivity and diffusivity, are important in the prediction of the depth of the cryosphere, which is the region where the temperature remains below the freezing point of water. A knowledge of the thermal conductivity of the soil of comets is important in the physical interpretation of the thermal evolution of comets. The effective thermal conductivity of a porous medium is dependent on a wide variety of properties related to the porous medium, including mineral composition of the solid particles, dry density, porosity, temperature, and water content, in liquid and solid phases. A theoretical prediction of the thermal conductivity can be used to determine also the thermal diffusivity, from a knowledge of the density and the specific heat.

Several experimental measurements on soils have been carried out at moderately high temperatures [1–5]. The soils measured span different types, varying in mineral composition, dry density, porosity, and water content. Experimental measurements of the thermal conductivity of two-phase porous media have been done, with the method of the thermal probe, on insulating materials [6], glass beads [7], and dry olivine, with solid particles with diameters smaller than 0.074 mm [8].

A review of the literature has revealed that theoretical models proposed for unsaturated porous medium are few. Two papers [9, 10] compared some modeling approaches to predict the effective thermal conductivity of soils at moderately high temperatures. The theoretical model, originally proposed in Ref. 11 for four-phase soils, in partially frozen conditions, has been later tested with bricks [12]. A model for the thermal conductivity of unconsolidated porous medium, based on a capillary pressure-saturation relation, has been proposed in Ref. 13. The stagnant thermal conductivity of spatially periodic porous media has been studied in Ref. 14. Two models have been developed to predict the effective thermal conductivity of consolidated porous media like cellular ceramics [15]. A model to determine the thermal conductivity of a bed of solid spherical particles immersed in a static fluid, when the thermal conductivity of the solid matrix is greater than that of the gas, has been formulated in Ref. 16.

The present paper reports experimental measurements on three-phase olivine, and air-water-olivine, with diameters of the solid particles in the range of 0.8 to 1 mm. Furthermore, the paper extends the theoretical model, called the cubic cell model, already employed in Refs. 7–12 with three- and four-phase media, tested with experimental data in Refs. 17 and 18, and extended to include thermal radiation in Refs. 19 and 20.

2. EXPERIMENTAL SETUP

The thermal probe is made from a hollow cylinder with a length of 59.1 mm, an external diameter of 0.6 mm, and an internal diameter of 0.3 mm, containing a platinum heating wire (total electrical resistance of 5.8 W) with a diameter of 65 μm and a copper-constantan thermocouple with a diameter of 76 μm. An epoxy resin is put inside the cylinder to keep the heating wire and the thermocouple stable. The handle of the probe is made with the same epoxy resin. The probe is shown in Fig. 1. Other details of the probe can be found in Ref. 8.

The thermal probe is positioned on the axis of a cylindrical container, at a height of 70 mm and with a diameter of 70 mm, where olivine is present. A second thermocouple is placed on the wall of the container in order to control the global heating of olivine. The container is maintained at constant temperature during the experiment by circulating ethyl glycol, at the prescribed temperature of the experiment, through the use of a cryostat. The container, with olivine, thermal probe, and instrumentation, is shown in Fig. 2.

The electric platinum wire is supplied with a constant current source (Kepco bipolar operational power supply/amplifier). At the beginning of the process, time $t = 0$, the electric current is switched on, giving a constant heat dissipation inside the probe. The temperature of the thermal probe thermocouple and that on the container wall are monitored by a data acquisition system.

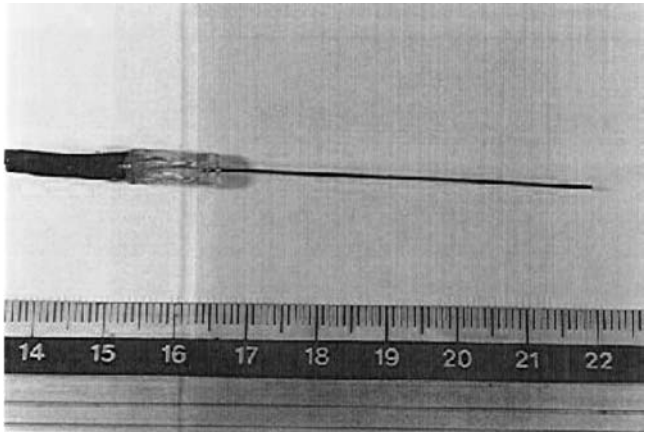

Fig. 1. Thermal probe.

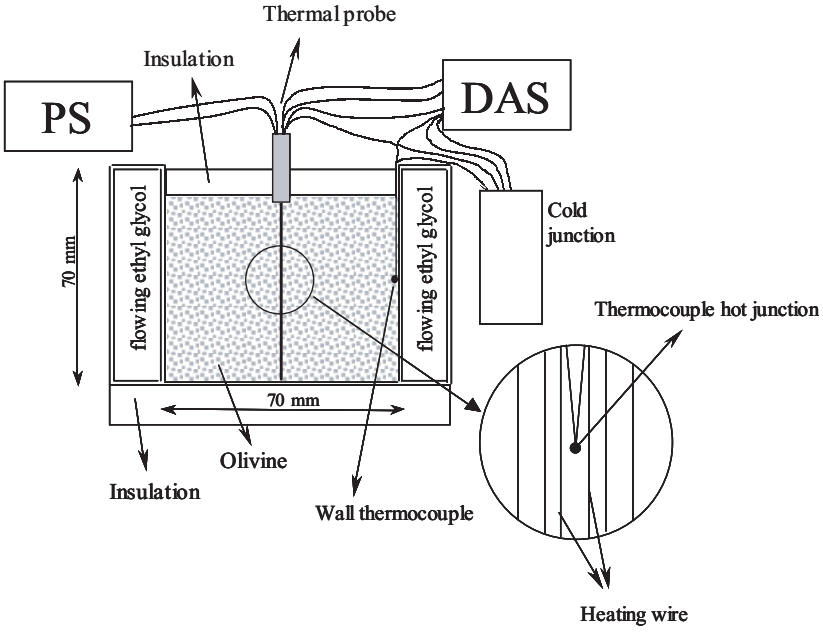

Fig. 2. Container with the olivine, thermal probe, and instrumentation.

3. EXPERIMENTAL RESULTS

The effects of the finite dimensions of the thermal probe have been tested according to the error analysis of Refs. 21 and 22. Thomas and Ewen [22] studied the effects of the error, in the measurement of the thermal conductivity, as a function of the thermal diffusivity of the sample, probe radius, heat capacities of the probe relative to the sample, ratio of outer to inner radius of the probe and contact resistance. The error is given by the following equation:

$$\text{error} = \frac{r^2}{2\alpha t}\left[(1-\phi)\left(0.5772 - \ln\frac{4\alpha t}{r^2}\right) - \phi + \frac{2\phi K_m}{rH}\right] \tag{1}$$

where

$$\phi = \frac{(\rho c)_p}{(\rho c)_m}[1-(a/r)^2].$$

The error due to the probe dimensions has been found to be 3.6%. The probe has been calibrated using test liquids such as glycerol and ethyl glycol. The thermal conductivity of glycerol has been measured with a deviation of 4.2% from the literature value at 25°C ($0.286\,W \cdot m^{-1} \cdot K^{-1}$) while ethyl glycol has been measured with a deviation of 1.7% from the standard value ($0.256\,W \cdot m^{-1} \cdot K^{-1}$) at 25°C.

Olivine, with particles of diameter in the range of 0.8 to 1 mm, has been tested in a dry condition over the range of temperatures from −17° to +50°C. Figure 3 presents the temperature increase of the thermal probe versus time in dry olivine at an initial temperature of −17°C. The temperature of the probe increases by less than 6°C. The temperature at the wall of the container has been monitored in order to show that, in the time range considered, the assumption of an infinite medium is valid because it remains almost constant.

The effective thermal conductivity has been calculated according to the perfect line source theory [23]. The presence of a linear slope in the increase of the probe temperature, on a semi-logarithmic plot, as shown in Fig. 3, is evidence of good performance of the thermal probe used for the measurement. The slope is determined through a regression least-squares analysis. In the experiment with dry olivine, Fig. 3, the estimated thermal conductivity is $0.149\,W \cdot m^{-1} \cdot K^{-1}$.

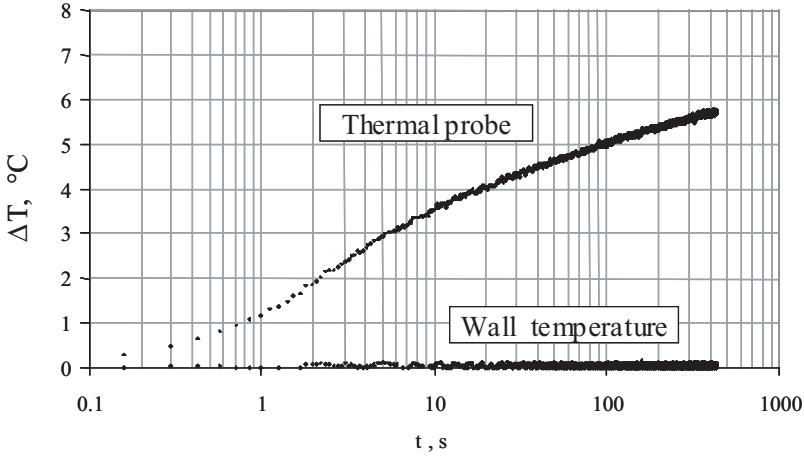

Fig. 3. Experimental temperature increase in the probe and at the container wall in dry olivine at −17°C.

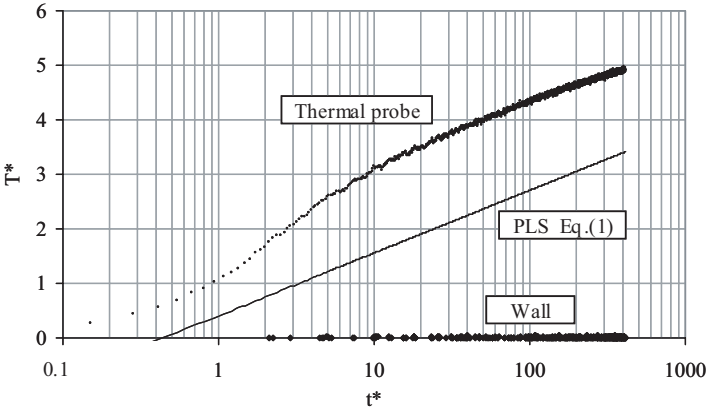

Fig. 4. Dimensionless temperature increase on the probe, at the container wall, in dry olivine, and perfect line solution (PLS).

The experimental data of Fig. 3 have been reported in dimensionless form in Fig. 4, along with the theoretical results given by the perfect line source (PLS) equation:

$$T^* = 0.5[\ln(4t^*) - 0.5772]. \tag{2}$$

The calculated value of the thermal conductivity is used to find the slope of the experimental dimensionless results. With a few iterations, it is possible to find the value of the thermal conductivity which gives a slope equal to 0.5, as expected from Eq. (2), with a high degree of accuracy.

Figure 4 shows the perfect line source (PLS) results, the experimental data, and the wall temperature in dimensionless form. The experimental data are higher than the results of the PLS solution because of the epoxy resin present inside the probe, which produces a temperature difference across its layer. The influence of the internal layer of epoxy resin has been discussed in Ref. 8, where three different configurations of the materials inside the probe have been suggested.

The experimental effective thermal conductivity of dry olivine has been measured in the range of temperatures between $-17°$ and $+50°C$. Figure 5 reports the experimental data along with experimental uncertainties and the interpolating line.

The temperature increase of the thermocouple in the probe and at the container wall has been measured in water-saturated olivine. The measurements are reported in Fig. 6 for a test at an initial temperature of

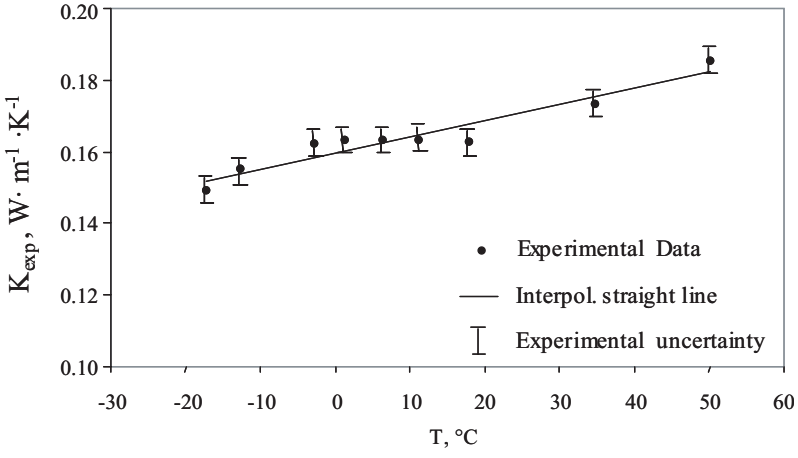

Fig. 5. Experimental effective thermal conductivity of dry olivine versus temperature.

+50°C. The experiments show a temperature increase in the probe of less than 1.1 K. In the experiment of Fig. 6, the estimated value of the effective thermal conductivity is 1.70 $W \cdot m^{-1} \cdot K^{-1}$.

The experimental data of Fig. 6 have been reported in dimensionless form in Fig. 7, along with the theoretical results given by the PLS solution,

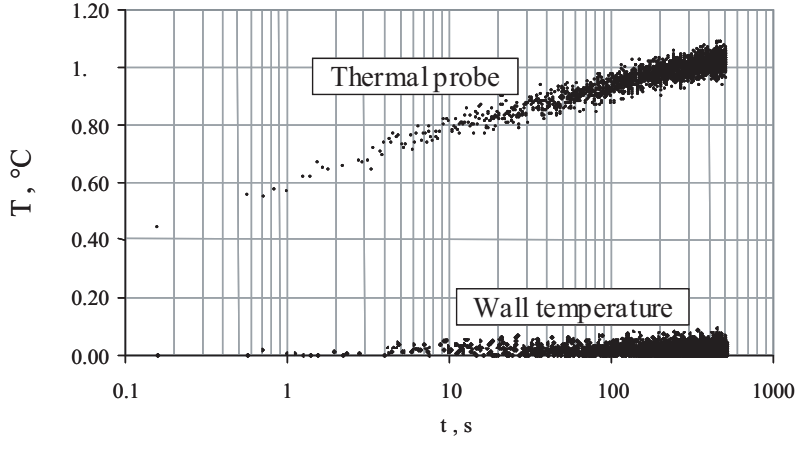

Fig. 6. Experimental temperature increase in the probe and at the container wall in water-saturated olivine at 50°C.

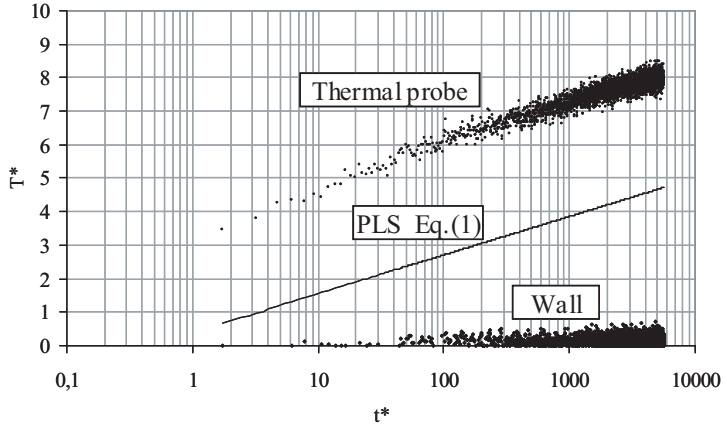

Fig. 7. Dimensionless temperature increase on the probe and at the container wall, in water-saturated olivine, and perfect line solution (PLS).

Eq. (2). The calculated value of the thermal conductivity is used to find the slope of the experimental dimensionless results. With a few iterations, it is possible to find the value of the thermal conductivity, which gives a slope equal to 0.5, as expected from Eq. (2), with a high degree of accuracy.

The effective thermal conductivity of water-mixed olivine has been measured at $+50°C$ for several levels of water saturation. The experimental results are reported in Fig. 8 versus the degree of saturation, φ, from complete dryness to full saturation. At $+50°C$ the effective thermal conductivity changes from about $0.2\,W \cdot m^{-1} \cdot K^{-1}$, at complete dryness, to about $1.7\,W \cdot m^{-1} \cdot K^{-1}$, at full saturation.

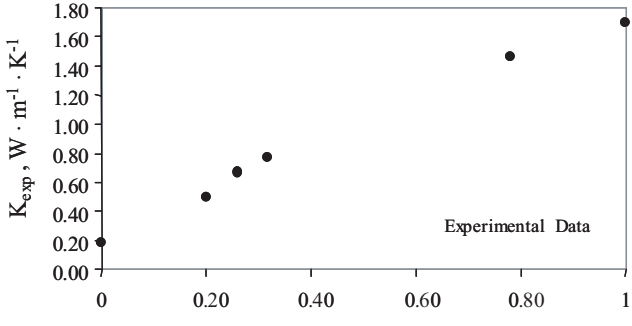

Fig. 8. Effective thermal conductivity of olivine at 50°C and several levels of saturation.

4. THEORETICAL PREDICTIONS OF THE EFFECTIVE THERMAL CONDUCTIVITY

4.1. Two-Phase Porous Media

The theoretical method, proposed in Ref. 11 and tested in Refs. 7–10, 12, and 17–20, assumes the two-phase porous medium is represented by a cubic space, with the solid particle in the form of a cubic cell at the center and the fluid surrounding it. With the assumption of parallel isotherms (very high thermal conductivity in the transverse direction), the effective thermal conductivity can be calculated by the solution of the heat conduction equation which gives the following expression:

$$\frac{1}{K_T} = \frac{1}{K_c}\frac{\beta-1}{\beta} + \frac{\beta}{K_c(\beta^2-1)+K_s} \tag{3}$$

K_c is the thermal conductivity of the fluid, K_s of the solid particle, and the parameter β is related to the porosity ε of the medium by the expression,

$$\beta = \sqrt[3]{\frac{1}{1-\varepsilon}}. \tag{4}$$

The evaluation of the thermal conductivity of the solid particle is a very difficult task in soils because it is highly dependent on the chemical composition of the solid, and it requires a measurement of the mineral composition of the investigated soil. In order to avoid such a measurement procedure, the following approach has been used.

Equation (3) has been employed two times, employing the measured effective thermal conductivity in a dry condition, K_{dry}, and in a water-saturated condition, K_{sat}. In this way two equations are available with two unknowns, which are the porosity of the porous medium, ε, or the related parameter, β, and the thermal conductivity of the solid grain, K_s. The two values used for the present solution are the average value measured in dry olivine, as found from Fig. 5, which is equal to $K_{dry} = 0.149\ W \cdot m^{-1} \cdot K^{-1}$, and the value measured in water-saturated condition, which is equal to $K_{sat} = 1.70\ W \cdot m^{-1} \cdot K^{-1}$. The resulting values are $\varepsilon = 0.37$ for the porosity and $K_s = 2.94\ W \cdot m^{-1} \cdot K^{-1}$ for the solid particle thermal conductivity.

The porosity in the bulk of the porous medium has been measured as $\varepsilon = 0.32$, and some analysis must be done in order to make a direct comparison with the predicted value of $\varepsilon = 0.37$. The use of a thermal probe, with a diameter smaller than the diameter of the particles of the porous medium where it is inserted, gives a lower thermal conductivity near the probe surface than in the core of the medium, because of the air layer

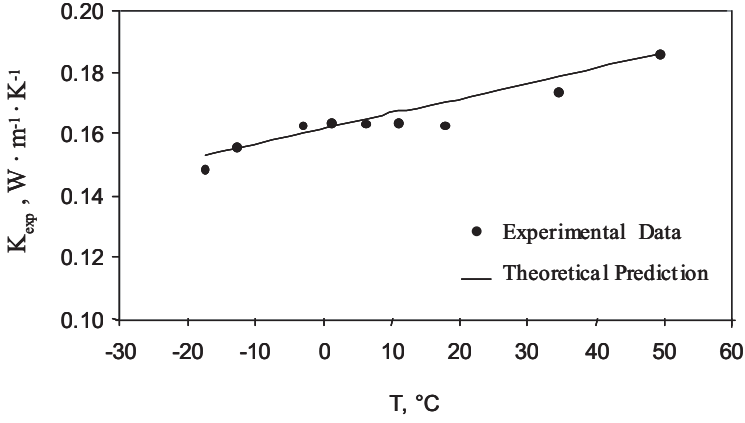

Fig. 9. Comparison between theoretical predictions and experimental data for dry olivine.

between the thermal probe and the porous medium [7]. The porosity of the porous medium near the thermal probe can be calculated according to the theoretical approach of Ref. 24. Assuming that the diameters of the solid particles of the porous medium are in the range between 0.8 and 1 mm, application of the following equation [24]:

$$\varepsilon_{corr} = \varepsilon_{exp} \lfloor 2.778 - 1.778 \exp(-d/D) \rfloor \tag{5}$$

gives porosities, in the vicinity of the probe, in the range of $\varepsilon = 0.39$ to 0.40, for 0.8 mm and 1 mm particles. Thus, the porosity corrected by the theoretical approach of Ref. 24, $\varepsilon = 0.39$ to 0.40, and the porosity from the use of Eq. (3), in dry and saturated conditions, which is $\varepsilon = 0.37$, are in reasonable agreement.

The porosity value of $\varepsilon = 0.37$ and $K_s = 2.94\ \mathrm{W \cdot m^{-1} \cdot K^{-1}}$ have been used to calculate, with Eq. (3), the effective thermal conductivities of dry olivine, at the temperatures of the measurements reported in Fig. 5. Theoretical predictions are reported in Fig. 9, which are in good agreement with the experiments.

4.2. Three-Phase Porous Media

Theoretical predictions of the thermal conductivity of a three-phase porous medium can be done with the cubic cell model assuming a certain distribution of the water around the cubic particle. Such a distribution of water must take into account the phenomena of absorption and capillarity and is summarized by the configurations of Figs. 10a to 10d.

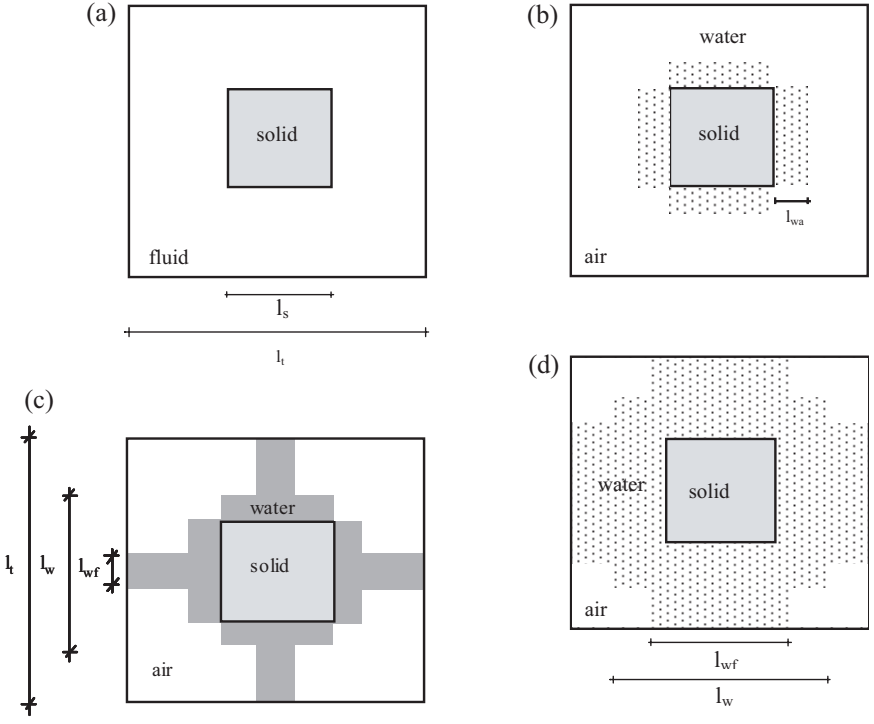

Fig. 10. (a) Unit cell of porous; (b) Water adsorbed around the solid particle; (c) Cubic cell model with water around the solid particle, according to absorption and capillarity among the adjacent particles; (d) Water adsorbed around the solid particle and disposed among adjacent particles.

For dry and water-saturated olivine only two phases are present, the solid particle and the fluid (air and water). In a three-phase olivine system, the water distribution is different according to the amount of water content. If the water content W is lower than $W_a = 0.083$, which is an empirical value proposed in Ref. 11, the water is adsorbed around the solid particle and no water bridges are established among the adjacent particles, Fig. 10b. In this case the effective thermal conductivity is given by

$$\frac{1}{K_T} = \frac{\beta - 1 - \delta/3}{\beta K_c} + \frac{\beta \cdot \delta}{3[K_c(\beta^2 - 1) + K_w)]} + \frac{\beta}{K_s + \frac{2}{3}\delta K_w + K_c\,(\beta^2 - 1 - \frac{2}{3}\delta)} \tag{6}$$

where

$$\delta = \frac{W}{1-\varepsilon} = 6\frac{l_{wa}}{l_s}. \tag{7}$$

If $W > W_a$, Figs. 10c and d, the amount of water accumulated among the solid particles is the funicular one, $\frac{v_{wf}}{V_s}$ according to Ref. 25. In order to simplify the model, $\frac{v_{wf}}{V_s}$ is assumed linearly proportional to the real porosity of the porous medium between 0.183, for $\varepsilon = 0.4764$, and 0.226, for $\varepsilon = 0.2595$. The resulting expression is:

$$\frac{V_{wf}}{V_s} = \frac{V_{wf}}{V_v}(\beta^3 - 1) = \left[0.183 + \frac{0.226 - 0.183}{0.4764 - 0.2595}(0.4764 - \varepsilon)\right](\beta^3 - 1). \quad (8)$$

The following variables are then defined:

$$\gamma = \frac{l_w}{l_s} = \sqrt[3]{\frac{V_w}{V_s} - \frac{V_{wf}}{V_s} + 1} \quad (9)$$

$$\gamma_f = \frac{l_{wf}}{l_s} = \sqrt{\frac{V_{wf}/V_s}{3(\beta - \gamma)}}. \quad (10)$$

In the configuration of Fig. 10c, where $\gamma_f < 1$, K_T is given by

$$\frac{1}{K_T} = \frac{\beta^{2\cdot} - \beta\gamma}{K_c(\beta^2 - \gamma_f^2) + K_w\gamma_f^2} + \frac{\beta\cdot\gamma - \beta}{K_c(\beta^2 - \gamma^2) + K_w\gamma^2} + \frac{\beta - \beta\gamma_f}{K_c(\beta^2 - \gamma^2) + K_w(\gamma^2 - 1) + K_s} + \frac{\beta\gamma_f}{K_s + K_w(\gamma^2 - 1 + 2\beta\gamma_f - 2\gamma\gamma_f) + A} \quad (11)$$

where $A = K_c(\beta^2 - \gamma^2 - 2\beta\gamma_f + 2\gamma\gamma_f)$.

For $\gamma_f > 1$, Fig. 10d, K_T has the following expression:

$$\frac{1}{K_T} = \frac{\beta^{2\cdot} - \beta\gamma}{K_c(\beta^2 - \gamma_f^2) + K_w\gamma_f^2} + \frac{\beta\gamma - \beta\gamma_f}{K_c(\beta^2 - \gamma^2) + K_w\gamma^2} + \frac{\beta\gamma_f - \beta}{K_c(\beta^2 - \gamma^2 - 2\beta\gamma_f + 2\gamma\gamma_f) + K_w(\gamma^2 + 2\beta\gamma_f - 2\gamma\gamma_f)} + \frac{\beta}{K_s + K_w(\gamma^2 - 1 + 2\beta\gamma_f - 2\gamma\gamma_f) + K_c(\beta^2 - \gamma^2 - 2\beta\gamma_f + 2\gamma\gamma_f)}. \quad (12)$$

Theoretical predictions of the previous equations are presented in Fig. 11, along with the experimental results at +50°C. The general agreement is good. There is only some overprediction in the range of water content from dryness to about 0.30 but it is considered sufficient since the value of 0.083 is the only empirical constant.

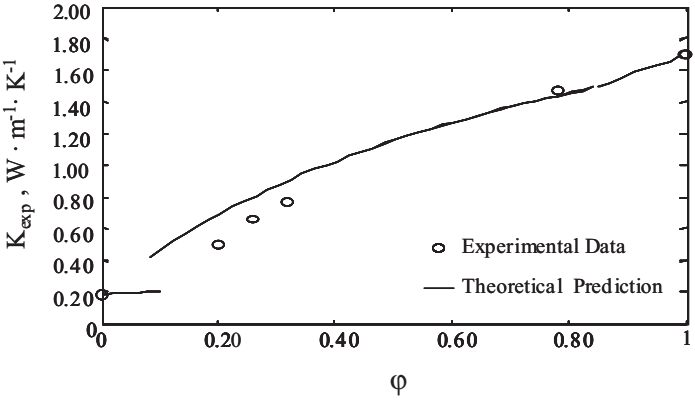

Fig. 11. Comparison between theoretical predictions and experimental data for olivine at various levels of saturation, from dryness to saturation, at 50°C.

5. CONCLUSIONS

Thermal conductivity measurements were carried out on olivine with particle diameters in the range between 0.8 and 1 mm, dry and water-mixed, up to full saturation. Dry olivine has been tested between −17° and +50°C. Olivine mixed with water has been measured at +50°C from complete dryness to full saturation. The cubic cell model has been used to predict the thermal conductivity of dry and water-mixed olivine with good agreement with measured values. For the case of olivine mixed with water, the cubic cell model has been used to evaluate the thermal conductivity of the solid particle and the porosity near the probe surface. The predicted porosity has been found in reasonable agreement to the measured value in the core of the porous medium and to the value predicted theoretically when the probe has a diameter smaller than that of the solid particles.

NOMENCLATURE

Latin Symbols

a internal probe radius (m)
c specific heat ($J \cdot kg^{-1} \cdot K^{-1}$)
d particle diameter (m)
D external probe diameter (m)
H conductance at the probe/sample interface ($W \cdot m^{-2} \cdot K^{-1}$)

K thermal conductivity ($W \cdot m^{-1} \cdot K^{-1}$)
l cubic cell length (m)
L probe length (m)
q heat flux (W)
$T^* = \frac{K \Delta T 2\pi L}{q}$ dimensionless temperature
T temperature (K)
$t^* = \frac{\alpha t}{r^2}$ dimensionless time
r external probe radius (m)
t time (s)
V volume (m^3)
W water content ($m^3 \cdot m^{-3}$)

Greek Symbols

α thermal diffusivity ($m^2 \cdot s^{-1}$)
$\beta = \frac{l_t}{l_s}$ length ratio
ρ bulk density ($kg \cdot m^{-3}$)
$\delta = \frac{W}{1-\varepsilon}$ dimensionless quantity
Δ finite difference
$\varepsilon = \frac{V_v}{V_t}$ porosity
φ saturation degree
$\gamma = \frac{l_w}{l_s}$ length ratio
$\gamma_f = \frac{l_{wf}}{l_s}$ length ratio
ρ density ($kg \cdot m^{-3}$)

Subscripts

a adsorbed
c continuous phase
corr corrected
d dry
dry dryness
exp experimental
m medium
p probe
s solid phase
sat saturation
T parallel isotherm
t total
v void
w water
wa adsorbed water
wf funicular water

ACKNOWLEDGMENT

The contribution of ASI (Italian Space Agency) to the program VIRTIS-Rosetta, coordinated by Dr. Angioletta Coradini, is gratefully acknowledged.

REFERENCES

1. G. S. Campbell, J. D. Jungbauer, W. R. Bidlake, and R. D. Hungerford, *Soil Sci.* **158**:307 (1994).
2. D. A. de Vries, *Physics of Plant Environment*, W. R. Van Wijk, ed. (John Wiley, New York, 1963), pp. 210–235.
3. A. R. Sepaskhah and L. Boersma, *Soil Sci. Soc. Am. J.* **43**:439 (1979).
4. J. W. Hopmans and J. H. Dane, *Soil Sci.* **142**:187 (1986).
5. Y. Hiraiwa and T. Kasubuchi, *Eur. J. Soil Sci.* **51**:211 (2000).
6. F. Gori and M. Pietrafesa, *ASME-WAM, HT-7A-5 or HTD, Vol. 179, Fundamental Experimental Measurements in Heat Transfer,* D. E. Beasley and J. L. S. Chen, eds., H00663-1991 (Atlanta, Georgia, 1991), pp. 83–89.
7. F. Gori, C. Marino, and M. Pietrafesa, *Int. Commun. Heat Mass* **28**:1091 (2001).
8. F. Gori and S. Corasaniti, *5th World Conf. Exp. Heat Transfer, Fluid Mechanics Thermodyn.* **2**:1257 (2001).
9. V. R. Tarnawski, F. Gori, B. Wagner, and G. D. Buchan, *Int. J. Energ. Res.* **24**:403 (2000).
10. V. R. Tarnawski and F. Gori, *Int. J. Energ. Res.* **26**:143 (2002).
11. F. Gori, *Proc. Fourth Int. Conf. on Permafrost* (Fairbanks, Alaska, 1983), pp. 363–368.
12. F. Gori, *Proc. Eight Int. Heat Transfer Conf.* (San Francisco, California, 1986), pp. 627–632.
13. X. J. Hu, J. H. Du, S. Y. Lei, and B. X. Wang, *Int. J. Heat Mass Tran.* **44**:247 (2001).
14. C. T. Hsu, P. Cheng, and K. W. Wong, *J. Heat Transf.* **117**:264 (1995).
15. X. Fu, R. Viskanta, and J. P. Gore, *Int. Commun. Heat Mass* **25**:151 (1998).
16. A. J. Slavin, F. A. Londry, and J. Harrison, *Int. J. Heat Mass Tran.* **43**:2059 (2000).
17. F. Gori and S. Corasaniti, *IMECE, International Mechanical Engineering Congress and Exposition, HTD-24152, ASME* (2001), pp. 1–8.
18. F. Gori and S. Corasaniti, *J. Heat Tran., ASME* **124**:1001–1008 (2002).
19. F. Gori and S. Corasaniti, *Proc. 19th UIT Nat. Heat Transfer Conf.* (2001), pp. 371–376.
20. F. Gori and S. Corasaniti, *Microgravity and Space Station Utilization* **2**:23 (2001).
21. J. H. Blackwell, *Can. J. Phys.* **34**:412 (1956).
22. H. R. Thomas and J. Ewen, *J. Heat Transf.* **108**:705 (1986).
23. H. S. Carslaw and J. C. Jaeger, *Conduction of Heat in Solids* (Oxford University Press, London, 1959).
24. R. M. Fand and R. H. Yamamoto, *Proc. 9th Int. Heat Transfer Conf.*, Jerusalem, 15-PB-07 (1990).
25. A. V. Luikov, *Heat and Mass Transfer in Capillary-Porous Bodies* (Pergamon Press, Oxford, 1966).